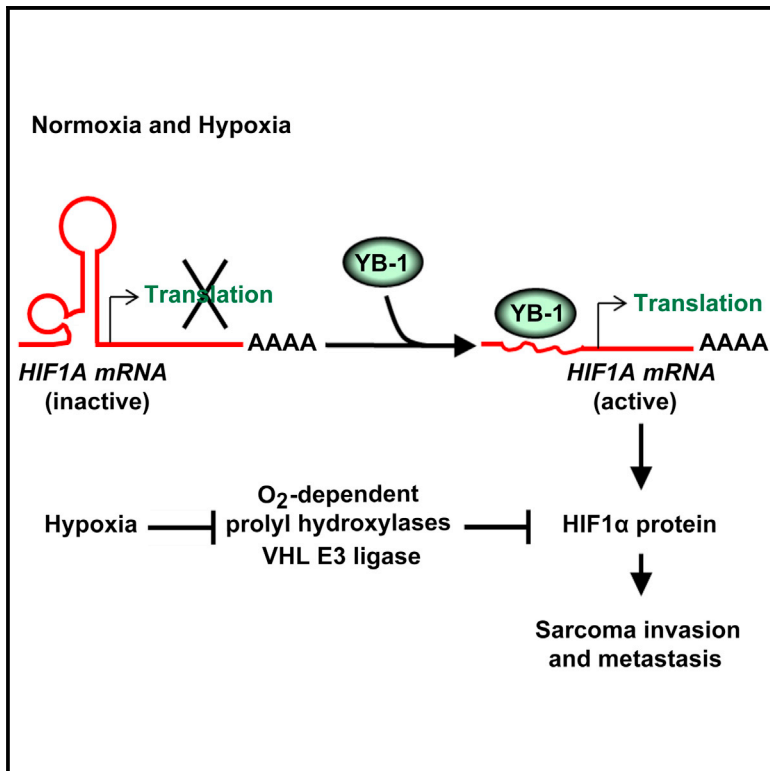


Translational Activation of HIF1 α by YB-1 Promotes Sarcoma Metastasis

Graphical Abstract



Authors

Amal M. El-Naggar,
Chansey J. Veinotte, ...,
Jason N. Berman, Poul H. Sorensen

Correspondence

psor@mail.ubc.ca

In Brief

YB-1 binds DNA and RNA and has been shown to promote epithelial-to-mesenchymal transition and metastasis of carcinomas. El-Naggar et al. show that YB-1 also contributes to metastasis of high-risk sarcomas by binding to *HIF1A* mRNA and enhancing its translation.

Highlights

- YB-1 expression is elevated in high-risk human sarcomas
- YB-1 promotes sarcoma invasion and metastasis
- YB-1 regulates HIF1 α expression by directly promoting its mRNA translation
- YB-1 effects on sarcoma invasion and metastasis are mediated by HIF1 α



Translational Activation of HIF1 α by YB-1 Promotes Sarcoma Metastasis

Amal M. El-Naggar,^{1,2} Chansey J. Veinotte,³ Hongwei Cheng,⁴ Thomas G.P. Grunewald,⁵ Gian Luca Negri,^{1,2} Syam Prakash Somasekharan,² Dale P. Corkery,³ Franck Tirode,⁶ Joan Mathers,² Debjit Khan,² Alastair H. Kyle,⁷ Jennifer H. Baker,⁷ Nancy E. LePard,⁷ Steven McKinney,² Shamil Hajee,² Momir Bosiljcic,^{1,7} Gabriel Leprivier,² Cristina E. Tognon,² Andrew I. Minchinton,⁷ Kevin L. Bennewith,^{1,7} Olivier Delattre,⁶ Yuzhuo Wang,⁴ Graham Dellaire,⁸ Jason N. Berman,^{3,8,9} and Poul H. Sorensen^{1,2,*}

¹Department of Pathology and Laboratory Medicine, University of British Columbia, Vancouver, BC V6T 2B5, Canada

²Department of Molecular Oncology, British Columbia Cancer Research Center, Vancouver, BC V5Z 1L3, Canada

³Department of Pediatrics, IWK Health Centre, Halifax, NS B3K 6R8, Canada

⁴Department of Urologic Sciences, University of British Columbia, Vancouver, BC V5Z 1M9, Canada

⁵Laboratory for Pediatric Sarcoma Biology, Institute of Pathology, LMU Munich, Thalkirchner Strasse 36, 80337 Munich, Germany

⁶INSERM U830, Laboratoire de génétique et biologie des cancers, Institut Curie, 75248 Paris, France

⁷Department of Integrative Oncology, Radiation Biology Unit, British Columbia Cancer Research Center, Vancouver, BC V5Z 1L3, Canada

⁸Department of Pathology

⁹Department of Pediatrics

Dalhousie University, Halifax, NS B3H 4R2, Canada

*Correspondence: psor@mail.ubc.ca

<http://dx.doi.org/10.1016/j.ccell.2015.04.003>

SUMMARY

Metastatic dissemination is the leading cause of death in cancer patients, which is particularly evident for high-risk sarcomas such as Ewing sarcoma, osteosarcoma, and rhabdomyosarcoma. Previous research identified a crucial role for YB-1 in the epithelial-to-mesenchymal transition (EMT) and metastasis of epithelial malignancies. Based on clinical data and two distinct animal models, we now report that YB-1 is also a major metastatic driver in high-risk sarcomas. Our data establish YB-1 as a critical regulator of hypoxia-inducible factor 1 α (HIF1 α) expression in sarcoma cells. YB-1 enhances HIF1 α protein expression by directly binding to and activating translation of *HIF1A* messages. This leads to HIF1 α -mediated sarcoma cell invasion and enhanced metastatic capacity in vivo, highlighting a translationally regulated YB-1-HIF1 α axis in sarcoma metastasis.

INTRODUCTION

Tumor metastasis is estimated to account for greater than 90% of cancer-related deaths (Gupta and Massagué, 2006). Sarcomas, malignancies of mesenchymal origin, have a particular propensity for local invasion and metastatic spread. For example, high-risk sarcomas, including Ewing sarcoma (EWS) and osteosarcoma (OS), the most frequent bone sarcomas, and rhabdomyosarcoma (RMS), the predominant childhood soft-tissue subtype, are characterized by early metastatic spread and poor prognosis (HaDuong et al., 2015). Although

important insights into sarcoma pathogenesis and molecular diagnostic tools have emerged, these findings have not impacted the prognosis for sarcoma patients with metastatic disease. Identifying factors that contribute to sarcoma metastasis and that can be targeted therapeutically thus has tremendous potential to significantly impact survival outcomes for patients having this group of diseases.

Y-box binding protein 1 (YB-1), which is encoded by *YBX1*, is a conserved protein that binds both DNA and RNA to orchestrate transcription as well as RNA processing and translation (Evdokimova et al., 2006a; Kohno et al., 2003). YB-1 plays prominent

Significance

Metastatic spread is the single-most powerful predictor of poor outcome in high-risk sarcomas. The lack of crucial insights into molecular mechanisms underlying metastatic capacity has severely hindered the development of effective strategies to improve therapeutic responses in these diseases. Our data establish YB-1 as a critical regulator of HIF1 α expression in sarcoma cells, leading to enhanced cell motility and metastatic capacity. Enhanced *HIF1A* mRNA translation by YB-1 under both normoxia and hypoxia provides an additional mechanism for regulating HIF1 α expression in tumors. Moreover, YB-1 also regulates HIF1 α expression in epithelial cancers. Our work highlights the potential for targeting the YB-1-HIF1 α cascade as a therapeutic strategy to prevent sarcoma metastasis, which could greatly impact outcomes for these diseases.

pro-oncogenic roles in malignant transformation, cell invasion, and drug resistance in a wide variety of cancers (Evdokimova et al., 2009; Giménez-Bonafé et al., 2004). YB-1 is a general suppressor of cap-dependent translation under diverse conditions (Evdokimova et al., 2006a; Somasekharan et al., 2012). However, some mRNAs are translationally activated by YB-1 under specific conditions. For example, we previously demonstrated that YB-1 blocks proliferation of breast cancer cells by repressing growth-related mRNAs such as cyclins, but simultaneously induces epithelial-to-mesenchymal transition (EMT) by directly binding to and activating translation of mRNAs encoding Snail1 and Twist EMT factors (Evdokimova et al., 2009). This is accompanied by enhanced metastatic capacity, and YB-1 is upregulated in invasive breast cancer and correlates with poor survival (Evdokimova et al., 2009). Notably, recent studies highlight YB-1 itself as being translationally induced downstream of mTORC1 signaling (Thoreen et al., 2012) and as a major translationally activated driver of mTORC1-mediated prostate cancer cell invasive capacity (Hsieh et al., 2012).

Intratumoral hypoxia is a common feature of solid malignancies, including sarcomas, hypoxia-inducible factor 1 α (HIF1 α), along with HIF2 α , is a requisite transcription factor for cellular adaptation to hypoxia, and both proteins can strongly influence the metastatic potential of tumor cells (Semenza, 2014). Indeed, HIF1 α has well-documented roles in cancer progression (Finger and Giaccia, 2010) and has been implicated in sarcoma metastasis (Eisinger-Mathason et al., 2013). Under hypoxia, HIF1 α is upregulated both transcriptionally (Belaiba et al., 2007) and through protein stabilization via functional inactivation of the Elongin B/C-CUL2-VHL E3 ligase complex, known to target HIF1 α for proteasomal degradation (Ivan et al., 2001; Jaakkola et al., 2001). However, the role of mRNA translation in regulating HIF1 α levels under hypoxia, particularly in tumor cells, is poorly understood, even though increased translation is estimated to account for 40%–50% of HIF1 α induction under hypoxia (Galbán et al., 2008; Hui et al., 2006).

Although many studies have revealed important roles for YB-1 in progression of epithelial cancers (Evdokimova et al., 2009; Gluz et al., 2009), its contribution in sarcomas is unknown, with only a few reports linking enhanced YB-1 expression to poor outcome in these diseases (Fujiwara-Okada et al., 2013; Xu et al., 2014). Because YB-1 induces an EMT and metastatic capacity in human breast cancer cells (Evdokimova et al., 2009), we wondered whether YB-1 might also promote metastatic behavior in sarcomas, which are already mesenchymal in origin.

RESULTS

YB-1 Is Elevated in High-Risk Sarcomas and Is Associated with Poor Outcome

We assessed *YBX1* mRNA expression in different human sarcoma subtypes from publically available datasets (see [Supplemental Experimental Procedures](#)). *YBX1* expression was higher across all sarcoma types analyzed compared with non-neoplastic tissues (Figure S1A). We then searched for sarcoma-related gene expression datasets with links to outcome, focusing on sarcoma subtypes with high metastatic rates (Ha-Duong et al., 2015). The GSE34620 dataset containing 117 cases (Postel-Vinay et al., 2012) revealed significantly higher *YBX1*

expression in metastatic compared with localized EWS (Figure 1A). Elevated *YBX1* expression also correlates significantly with higher mortality in EWS (Figure 1A), and high *YBX1* expression correlates with poor overall survival in EWS (Figure 1B). Elevated *YBX1* expression at diagnosis is also associated with reduced event-free survival in localized EWS (Figure S1B) and overall survival in metastatic EWS (Figure 1C). High *YBX1* levels are associated with reduced overall (Figure 1D) and event-free survival (Figure S1C) in OS and with reduced metastasis-free survival in synovial sarcoma (Figure 1E). High *YBX1* expression showed a trend toward reduced survival in RMS, though not significant because of small sample sizes (data not shown). Further supporting a role in metastatic disease, elevated *YBX1* expression also correlates with reduced overall and event-free or metastasis-free survival in breast cancer, clear cell renal cell carcinoma, and cervical carcinoma (Figures S1D–S1H). Strong cytoplasmic YB-1 staining by immunohistochemistry (IHC) was observed in RMS compared with adjacent normal skeletal muscle (Figure 1F) and in malignant OS cells compared with normal osteoblasts (OBs) (Figure S1I). YB-1 IHC on 25 OS cases using two independent YB-1 antibodies showed a correlation between elevated YB-1 expression and higher grade disease (Table S1). In EWS and OS cell lines, YB-1 levels were consistently elevated compared with normal OBs and in RMS cell lines compared with skeletal muscle (Figure 1G). Human fibroblasts and HEK293 cells showed lower YB-1 expression compared with TC32 EWS cells (Figure S1J). These data indicate that YB-1 expression is elevated in high-risk sarcomas and is associated with poor outcome.

YB-1 Increases Motility of Human Sarcoma Cells In Vitro and In Vivo

To determine how YB-1 contributes to aggressiveness of sarcomas, we first tested whether YB-1 increases cell migration in vitro, a critical feature of the metastatic phenotype (Chaffer and Weinberg, 2011). Given the high YB-1 expression in all sarcoma cell lines tested, we chose a YB-1 siRNA knockdown (KD) approach. Two or more independent siRNA sequences were used, leading to consistent YB-1 KD (Figure S2A). YB-1 KD significantly decreased MG63 OS cell migration in response to 10% fetal bovine serum (FBS), insulin, or insulin-like growth factor 1 (IGF1) (Figure 2A), and similarly reduced migration of MNNG OS and TC32 EWS cells (Figures 2B and S2B). These and RH30 cells migrate more rapidly than corresponding YB-1 KD cells in wound-healing assays (Figure S2C). YB-1 KD also significantly reduced invasive capacity in vitro, shown for CHLA10 EWS cells in Figure 2C, which was completely rescued by YB-1 re-expression using a siRNA-resistant expression plasmid. Moreover, in Matrigel 3D matrices, control TC71 EWS cell clusters displayed marked branching, whereas YB-1 KD clusters had rounded morphology characteristic of non-invasive cells (Figure S2D). Notably, YB-1 KD did not decrease proliferation rates of any of the cell lines used in this study (data not shown).

To confirm effects on motility in vivo, we adapted a zebrafish model, previously used to graft human leukemia cell lines into 48-hr embryos (Corkery et al., 2011), to xenotransplant TC32 cells into zebrafish embryos. TC32 cells were initially retained in the yolk sac and then rapidly migrated to tails of embryos within 120-hr post-injection (Figure 2D). Importantly, fixed

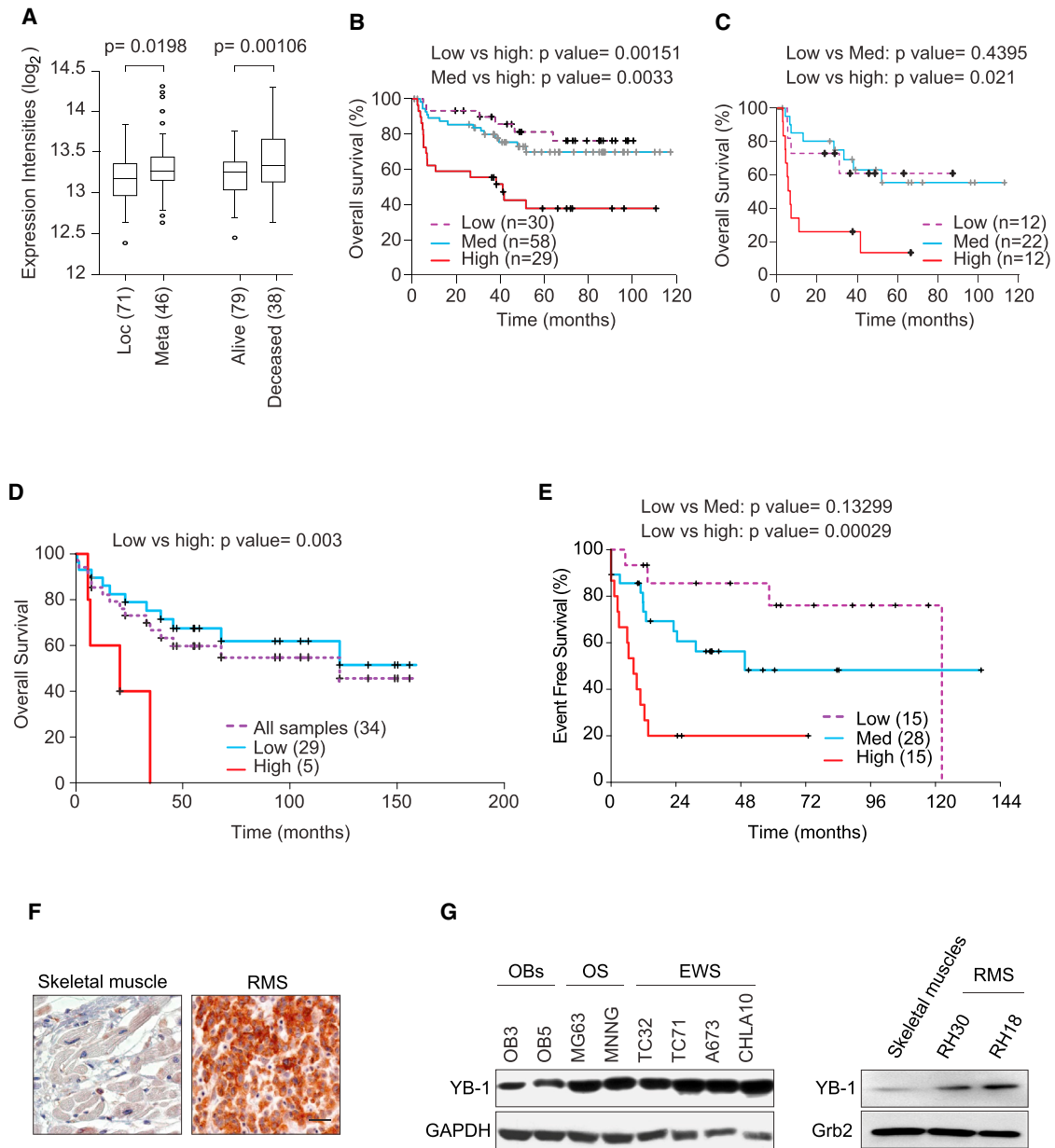


Figure 1. Elevated YB-1 Expression Is Predictive of Poor Outcome in Sarcoma Patients

(A) Correlation between *YBX1* mRNA level and metastatic disease or death in EWS patients using the GSE34620 database (n = 117) (Postel-Vinay et al., 2012). Associations were determined using a Welch t test and the two-sided p values are displayed. Data are presented as box plots. The bars indicate the medians, whereas the boxes represent the middle 50% of data points to graphically represent the interquartile range (IQR). The upper and lower whiskers represent the largest and smallest observed values that are less than 1.5 box lengths from the ends of each box. Round circles represent outliers.

(B) Kaplan-Meier curves of overall survival for EWS patients in the GSE34620 database based on *YBX1* expression, defined as low (25% of samples with lowest expression), high (25% with highest expression), and medium (50% of samples with medium expression).

(C) Impact of *YBX1* expression on overall survival (event = deceased) in EWS patients from the GSE34620 database with metastatic disease at diagnosis (n = 46).

(D) Kaplan-Meier curves showing the impact of *YBX1* expression on overall survival for OS patients (Man et al., 2005).

(E) Kaplan-Meier metastasis free survival curve for synovial sarcoma patients (Lagarde et al., 2013) showing the impact of *YBX1* expression on outcome.

(F) IHC staining for YB-1 expression in normal skeletal muscle and in RMS. Scale bars represent 100 μ m.

(G) Western blot showing YB-1 expression in benign primary OBs and in the indicated OS and EWS cell lines (left) or in skeletal muscles compared with the indicated RMS cell lines (right). GAPDH and Grb2 were used as loading controls.

See also Figure S1.

TC32 cells and inert microspheres failed to migrate, confirming that TC32 cell migration is an active rather than a passive process (Figure 2E). Migration into embryo tails of TC32 cells with

YB-1 KD was significantly reduced compared with controls (Figures 2D–2F and S2E), while their proliferation was similar to controls (Figure S2F). Similar results were obtained using a different

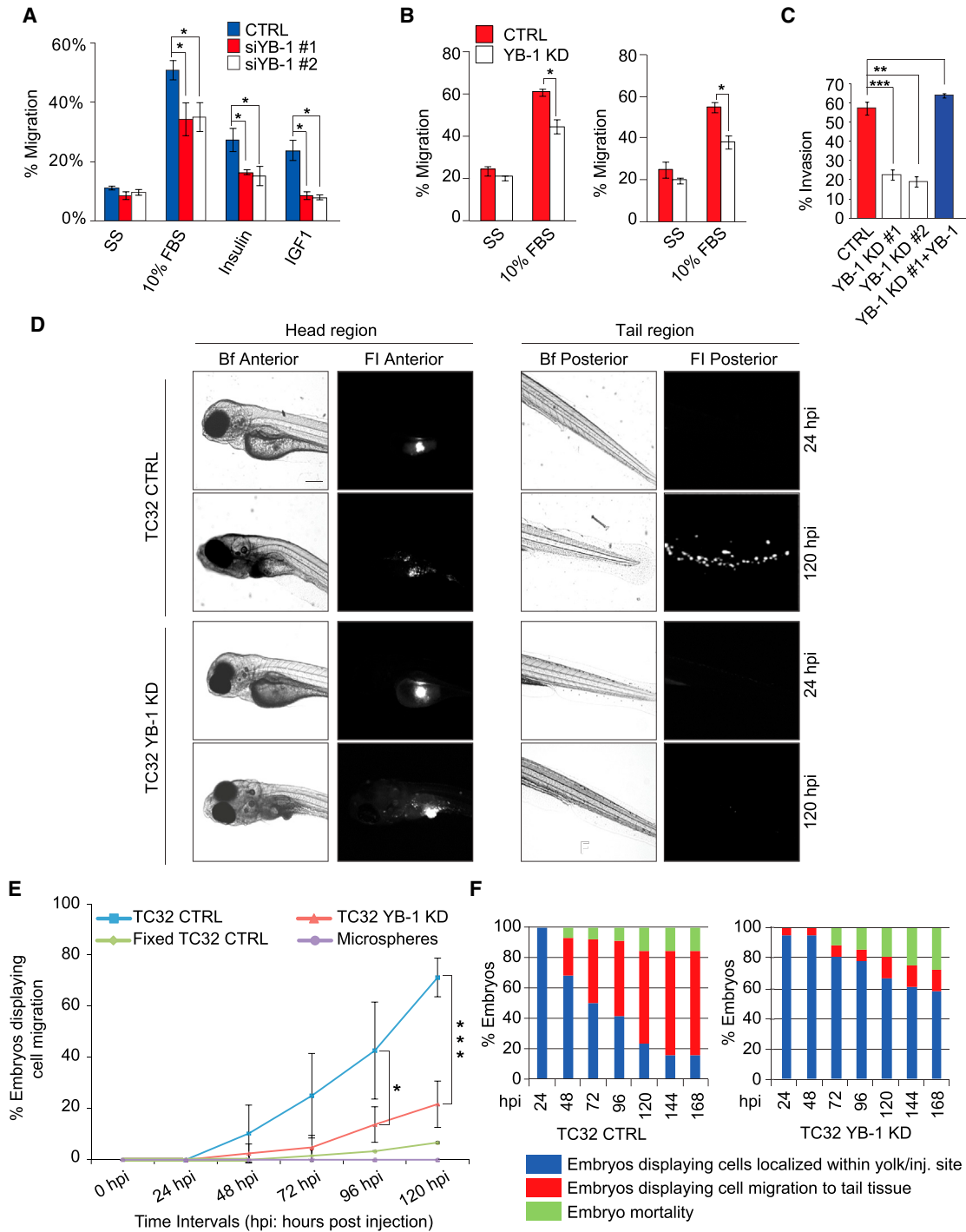


Figure 2. YB-1 Increases Sarcoma Cell Motility In Vitro and In Vivo

(A) Cell migration of MG63 OS cells ± YB-1 KD measured as percent cells migrating to chambers without serum; serum starved (SS), 10% FBS, 100 nM insulin, or 100 ng/ml IGF1. Results of two independent experiments in triplicate are presented as means ± SD.

(B) Cell migration of MNNG OS (left) and TC32 EWS cells (right) ± YB-1 KD, measured as percentage of cells migrating to chambers without serum (SS) or 10% FBS. The results of three independent experiments in triplicate are presented as means ± SD.

(C) In vitro invasion of CHLA10 EWS cells ± YB-1 KD and YB-1 KD cells with restored YB-1 expression (+YB-1). Results of two independent experiments in triplicate are shown as means ± SD.

(D) TC32 EWS cells ± YB-1 shRNA KD were labeled with Cm-Dil and injected into 48-hr post-fertilization (hpf) casper zebrafish embryos. Bright-field (Bf) and fluorescent (FI) live lateral images of the head (anterior) and tail (posterior) of embryos at 24- and 120-hr post-injection (hpi) are shown (n = 15–20 embryos). Scale bars represent 200 μm.

(legend continued on next page)

shRNA (YB-1 KD #2; [Figures S2G and S2H](#)), providing strong evidence that YB-1 increases cell motility of human sarcoma cells *in vivo*.

YB-1 Increases Sarcoma Cell Invasion and Metastasis *In Vivo*

To rigorously show that YB-1 facilitates aggressive behavior of sarcoma cells *in vivo*, we next used the murine renal subcapsular implantation model for establishing human tumor xenografts ([Bogden et al., 1979](#)). This system is advantageous due to extensive vascularization at the graft site and gives rise to quantifiable metastases of diverse human tumor cell lines ([Cutz et al., 2006](#)), including EWS cell lines ([Mendoza-Naranjo et al., 2013](#)). CHLA10, TC71, and TC32 EWS cell lines \pm stable shRNA-mediated YB-1 KD were luciferase (LUC) labeled and implanted under the renal capsules of immunocompromised mice and assessed for local growth and metastasis. Each cell line formed large tumors at primary implantation sites after several weeks (shown for TC32 cells in [Figure S3A](#)). There was no significant difference in gross sizes of primary tumors between control and YB-1 KD tumors ([Figure S3B](#)). Histology revealed small round cell tumors characteristic of EWS for each cell line ([Figure 3A](#)), confirmed by strong membranous IHC staining for the CD99 EWS biomarker ([Figure S3C](#)). YB-1 IHC confirmed reduced YB-1 levels *in vivo* in KD tumors ([Figure 3B](#)), with two independent shRNAs targeting YB-1 ([Figure S3D](#)). Supporting the above *in vitro* data, there was no significant difference in proliferative rates between control and YB-1 KD tumors determined by Ki-67 IHC ([Figure S3E](#)) or bromodeoxyuridine (BrdU) staining (data not shown).

Notably, control CHLA10, TC71, and TC32 tumors were highly infiltrative into adjacent normal kidney, whereas YB-1 KD tumors were non-invasive and had “pushing” borders abutting but not penetrating normal kidney ([Figure 3A](#)). Morphometric analysis revealed highly significant differences in invasion into adjacent normal kidney between control and KD tumors ([Figure S3F](#)). We then used morphology ([Figure 3C](#)) and CD99 IHC ([Figure S3G](#)) to screen for lung metastases. YB-1 KD significantly reduced the number of lung metastases per mouse for each cell line ([Figure 3D](#)) and the total mice with lung metastases ([Figures 3E and S3H](#)), with complete elimination of metastases in the CHLA10 group ([Figure 3D](#)). Similar results were obtained using an independent shRNA targeting YB-1 ([Figures 3F and S3D](#); YB-1 KD #2). Restoring YB-1 expression rescued metastatic capacity in the CHLA10 YB-1 KD group ([Figures 3F and 3G](#)). YB-1 overexpression in CHLA10 control cells ([Figures 3F and S3I](#)) led to slightly earlier metastatic spread (data not shown) but did not increase overall metastases, as 100% of mice in both groups eventually displayed lung metastases ([Figure 3G](#)). Of note, lung metastases that did form in the YB-1 KD group displayed strong YB-1 staining ([Figure 3H](#)), suggesting that in this group, metastatic tumors formed either from clones that had escaped initial YB-1 KD ([Figure S3J](#), see arrows) or that re-expressed YB-1

following initial silencing. Together, these findings provide compelling evidence that YB-1 confers invasive and metastatic capacity to sarcoma cells *in vivo*.

YB-1 Increases HIF1 α Protein Levels in Sarcoma Cells

YB-1 induces metastasis of breast cancer cells through *SNAI1* and *TWIST* translation ([Evdokimova et al., 2009](#)). However, *Snail1* was only very weakly expressed in the above sarcoma cell lines, while *Twist* was not consistently reduced by YB-1 KD (data not shown). We therefore wondered whether other EMT-associated transcription factors might be regulated by YB-1 in sarcomas. Compared with control renal subcapsular xenografts, tumors with YB-1 KD showed extensive hemorrhage and necrosis ([Figure 4A](#), asterisks; [Figures S4A and S4B](#)), typically found adjacent to areas of tumor hypoxia ([Höckel and Vaupe, 2001](#)). Indeed, there was extensive pimonidazole (pimo) staining in both control and YB-1 KD tumors, indicating that these lesions are hypoxic ([Figures 4B and 4C](#)), while adjacent normal kidney was negative ([Figures S4C and S4D](#)). Since the pro-angiogenic factor HIF1 α is stabilized in viable hypoxic tumor cells to regulate their survival under hypoxic stress and has well-documented roles in cancer progression ([Kaelin, 2011](#); [Semenza, 2003](#)), we wondered whether YB-1 might regulate HIF1 α expression. Indeed, HIF1 α protein levels were markedly reduced by YB-1 KD under 1% O₂ using two independent siRNAs in all sarcoma cell lines tested ([Figure 4D](#); data not shown). YB-1 KD blocked HIF1 α accumulation even under normoxia and after short-term growth at 1% O₂, as shown for MNNG cells in [Figure 4E](#). YB-1 KD also reduced HIF1 α expression under more stringent hypoxia at 0.2% O₂ ([Figure 4F](#)). Notably, YB-1 KD failed to reduce HIF2 α accumulation under hypoxia in MNNG and RH30 cells ([Figure S4E](#)) or in EWS cell lines (data not shown).

To validate this *in vitro*, we used the multilayered cell culture (MCC) system, in which an O₂ gradient is generated across 3D cultures of solid tumor cell lines ([Minchinton et al., 1997](#)). Using pimo staining to highlight hypoxia ([Figure S4F](#), left), YB-1 expression was largely limited to viable hypoxic regions adjacent to central necrotic cores in TC32 MCC aggregates ([Figure S4F](#), right). YB-1 was similarly expressed in control MNNG aggregates, which correlated with strong HIF1 α expression, but HIF1 α was significantly reduced by YB-1 KD ([Figure 4G](#)), further linking YB-1 to HIF1 α expression. Residual HIF1 α expression in YB-1 KD aggregates may be attributable to YB-1-independent HIF1 α regulation or to residual clones escaping initial KD or with shRNA silencing, as suggested in short-term MCC cultures ([Figure S4G](#)). Finally, YB-1 overexpression using Myc-tagged YB-1 in CHLA10 cells (see [Figure 3F](#)) moderately enhanced *in vitro* HIF1 α expression under both normoxia and hypoxia compared with controls ([Figure S4H](#)).

To confirm that YB-1-induced HIF1 α is biologically active, we monitored activity of a hypoxia response element (HRE) reporter linked to GFP in cells \pm YB-1 KD with two independent siRNAs. This revealed significantly higher HRE activity in control

(E) Cell migration to tail regions after xenotransplantation into casper embryos. TC32 control (CTRL) versus YB-1 KD cells were compared at 120 hpi with fixed TC32 CTRL cells and Tetraspeck microspheres as controls; n = 160–180 embryos per group. Error bars indicate SD.

(F) Migration of TC32 cells \pm YB-1 KD to tail regions after xenotransplantation into casper embryos and mortality at the indicated time points.

*p < 0.05, **p < 0.01, ***p < 0.001. hpi, hour post-injection. See also [Figure S2](#).

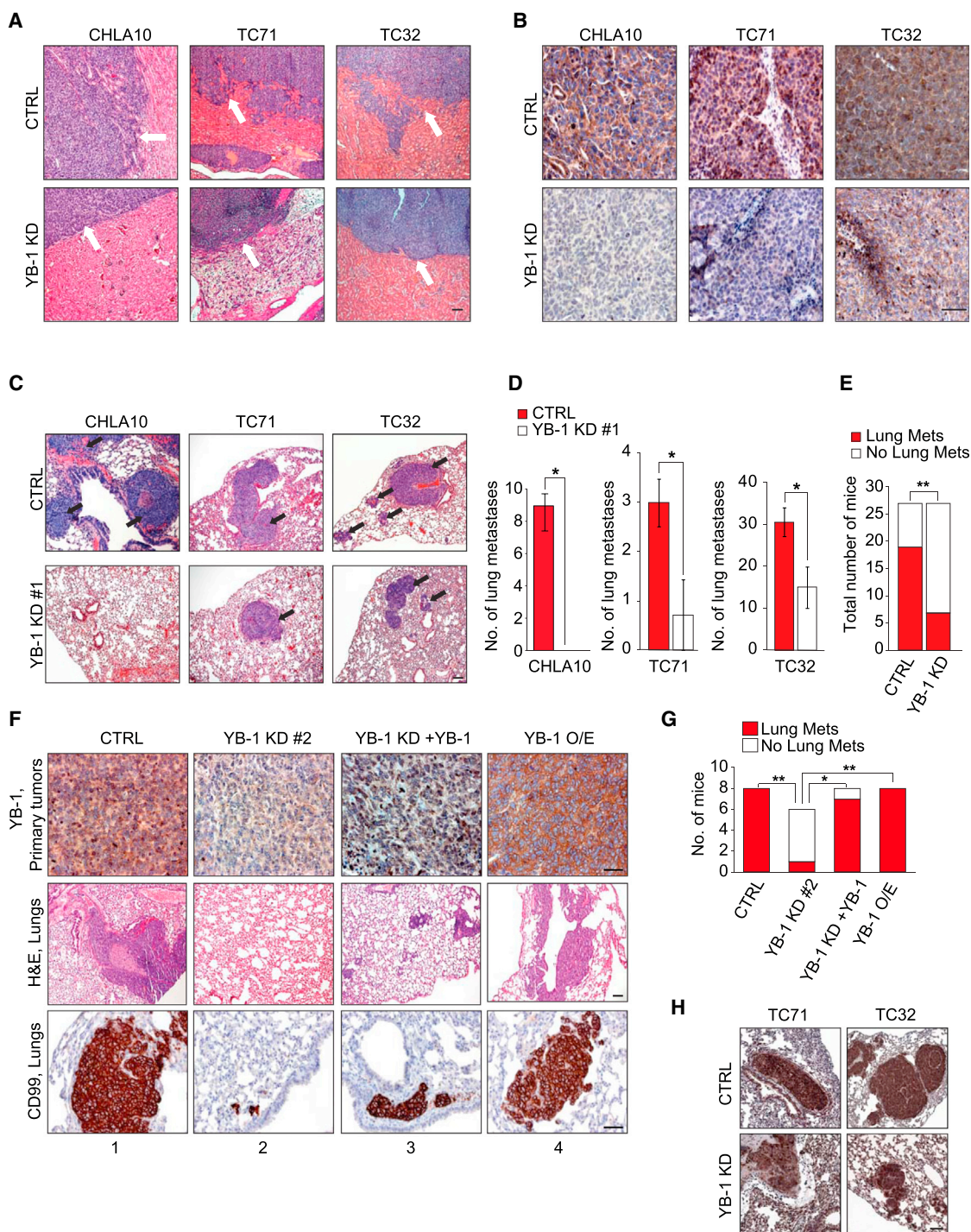


Figure 3. YB-1 KD Blocks Sarcoma Cell Metastasis In Vivo

(A) H&E-stained renal subcapsular primary tumor xenografts of CHLA10, TC71, and TC32 cell lines \pm YB-1 shRNA KD. White arrows in control (CTRL) and YB-1 KD tumors show tumor-normal kidney interfaces. Scale bars represent 100 μ m.

(B) IHC staining of YB-1 in primary tumor xenografts of the indicated EWS cell lines \pm shRNA YB-1 KD. Scale bars represent 50 μ m.

(C) H&E staining of metastatic lung lesions (arrows) in mice with renal subcapsular tumor xenografts of the indicated EWS cell lines \pm shRNA YB-1 KD. Scale bars represent 100 μ m.

(D) Average number of lung metastases in mice bearing renal subcapsular tumor xenografts of CHLA10, TC71, and TC32 cell lines \pm shRNA YB-1 KD compared using a Wilcoxon two-sided rank sum test. Results are presented as mean \pm SEM.

(E) Total number of mice bearing xenografts of CHLA10, TC71, and TC32 cell lines \pm shRNA YB-1 KD that developed lung metastases, determined using a Fisher's exact test.

(legend continued on next page)

compared with RH30 YB-1 KD cells under both normoxia and hypoxia (Figure 4H). Next, we analyzed lysates from renal subcapsular xenografts of MNNG cells \pm YB-1 KD for HIF1 α expression and found markedly reduced HIF1 α protein levels in KD tumors in vivo (Figure S4I). Consistent with this, tumor cryosections showed markedly reduced staining for the HIF1 α transcriptional target carbonic anhydrase IX (CAIX) (Wykoff et al., 2000) after YB-1 KD (Figure S4J). Therefore, YB-1 controls biologically active HIF1 α expression in sarcoma cell lines both in vitro and in vivo. Finally, to assess whether YB-1 regulates HIF1 α in human sarcomas, tissue microarrays (TMAs) from EWS (20 cases) and RMS (41 cases) were immunostained for YB-1 and HIF1 α . YB-1 expression strongly correlated with HIF1 α IHC in both EWS and RMS (Figures S4K and S4L; Tables S2 and S3). These data provide compelling evidence that YB-1 positively regulates HIF1 α protein expression in human sarcomas.

YB-1 Activates HIF1A Translation in Sarcoma Cells

We next determined how YB-1 regulates HIF1 α expression since YB-1 reportedly acts through both transcriptional and translational mechanisms (Eliseeva et al., 2011). We first compared total and polysome-bound (translationally active) HIF1A mRNA levels in cells \pm YB-1 KD by quantitative RT-PCR (qRT-PCR). Total HIF1A mRNA levels in hypoxic RH30 and MNNG cells either increased or stayed the same after YB-1 KD as in control cells (Figure 5A), arguing against a transcriptional mechanism for YB-1 induction of HIF1 α . In contrast, YB-1 KD significantly reduced the proportion of HIF1A transcripts in polysomal fractions (compare polysome levels \pm YB-1 KD in Figure 5A). Although HIF1A mRNA accumulation in polysomes was increased under hypoxia, YB-1 KD reduced this distribution under both normoxia and hypoxia (Figure 5B). In contrast, neither HIF2A mRNA levels nor its polysomal distribution was consistently affected by YB-1 KD under identical conditions (Figure S5A). This suggests that YB-1 enhances the proportion of HIF1A mRNAs undergoing active translation. To support this, we next monitored levels of newly synthesized HIF1 α in control versus YB-1 KD cells, using CLICK chemistry and L-azidohomoalanine (AHA) incorporation as described (Somasekharan et al., 2012). Hypoxic MNNG cells were pulsed with AHA, and AHA-labeled newly synthesized proteins were biotinylated and affinity purified with streptavidin. While control cells showed robust new synthesis of HIF1 α , this was almost completely blocked by YB-1 KD (Figure 5C). Together, these data indicate that YB-1 selectively increases HIF1A mRNA translation under both normoxia and hypoxia.

YB-1 Directly Binds to HIF1A mRNA to Control Its Translation

One explanation for these data is that YB-1 directly binds to and activates translation of HIF1A mRNAs, as described for

Snail and Twist (Evdokimova et al., 2009). Ribonucleoprotein (RNP) immunoprecipitation (RIP) with anti-YB-1 antibodies demonstrated that YB-1 associates with HIF1A transcripts in MNNG cells (Figure 5D). YBX1 and CCND1 transcripts, known to bind to YB-1 (Evdokimova et al., 2006b), were used as positive controls and RPL32 as a negative control (Evdokimova et al., 2006b). We then used a bicistronic reporter containing the full-length HIF1A 5'-UTR sequence cloned upstream of firefly LUC and Renilla LUC driven by the SV40 promoter (Bert et al., 2006) to assess whether the HIF1A 5'-UTR impacts YB-1-driven mRNA translation efficiency in cells. This revealed significantly higher LUC activity in MNNG control versus YB-1 KD cells (Figure 5E), indicating that in living cells, YB-1 facilitates translation of transcripts containing the HIF1A 5'-UTR. To directly test this, in vitro translation efficiencies of a LUC reporter linked to the 5'-UTR of either HIF1A (5'-HIF1A-LUC) or HBB (beta-globin) (5'-HBB-LUC) were tested using a cell-free transcription/translation system (Bert et al., 2006). As shown in Figure 5F, recombinant YB-1 at up to 0.6 pmol increased the translation efficiency of 5'-HIF1A-LUC, while minimally affecting translation of 5'-HBB-LUC. Above 0.6 pmol, YB-1 decreased translation from both 5'-UTRs, as reported for the SNAI1 5'-UTR (Evdokimova et al., 2009) and consistent with the known translational repressor function of YB-1 at high levels (Evdokimova and Ovchinnikov, 1999).

Supporting a role for YB-1 in controlling HIF1A translation efficiency, cross-species analysis reveals numerous conserved GC-rich sequences in the HIF1A 5'-UTR (Figure S5B), the favored YB-1 binding sequence (Eliseeva et al., 2011), particularly in nucleotides 133–257 of the human 5'-UTR. Vienna RNA secondary structure prediction tools (<http://ma.tbi.univie.ac.at/cgi-bin/RNAfold.cgi>) predict that the HIF1A 5'-UTR forms highly stable stem loop structures (Figure S5C) and thus may be susceptible to YB-1 helicase-mediated melting of its secondary structure, as described for the SNAI1 5'-UTR (Evdokimova et al., 2009). We therefore compared activity of the above WT HIF1A 5'-UTR-LUC reporter to that of deletion mutants lacking either nucleotides 1–130 (Δ 1–130) or 131–253 (Δ 131–254) of the HIF1A 5'-UTR. There was a marked reduction in YB-1-induced LUC activity for the Δ 131–254 mutant compared with the WT construct, which was less evident with the Δ 1–130 mutant (Figure 5G); YB-1 KD reduced activity of all three constructs. The same reporter substituted with WT HIF2A 5'-UTR was not activated by YB-1 (Figure 5G), consistent with YB-1 not affecting polysomal distribution of HIF2A mRNAs (Figure S5A). Finally, electrophoretic mobility shift assays (EMSAs) demonstrated direct binding of YB-1 to WT HIF1A 5'-UTR probe in a concentration-dependent manner (Figure 5H), which was completely inhibited with unlabeled probe. While both unlabeled Δ 1–130 and Δ 131–253 mutant probes reduced YB-1 binding to the

(F) (Upper) IHC staining for YB-1 in primary xenografts of CHLA10 cell line \pm YB-1 shRNA KD #2, YB-1 re-expression (+YB-1), or YB-1 overexpression (O/E). Scale bars represent 50 μ m. (Middle) H&E staining of metastatic lung lesions (arrows). Scale bars represent 100 μ m. (Lower) IHC staining of the EWS marker CD99 in lung tissues to highlight metastatic lesions. Scale bars represent 50 μ m.

(G) Total numbers of mice from (F) that developed lung metastases compared using a Fisher's exact test.

(H) IHC staining of YB-1 in lung metastases of mice bearing xenografts of TC71 and TC32 cell lines \pm shRNA YB-1 KD. Scale bars represent 100 μ m.

* $p < 0.05$, ** $p < 0.01$. See also Figure S3.

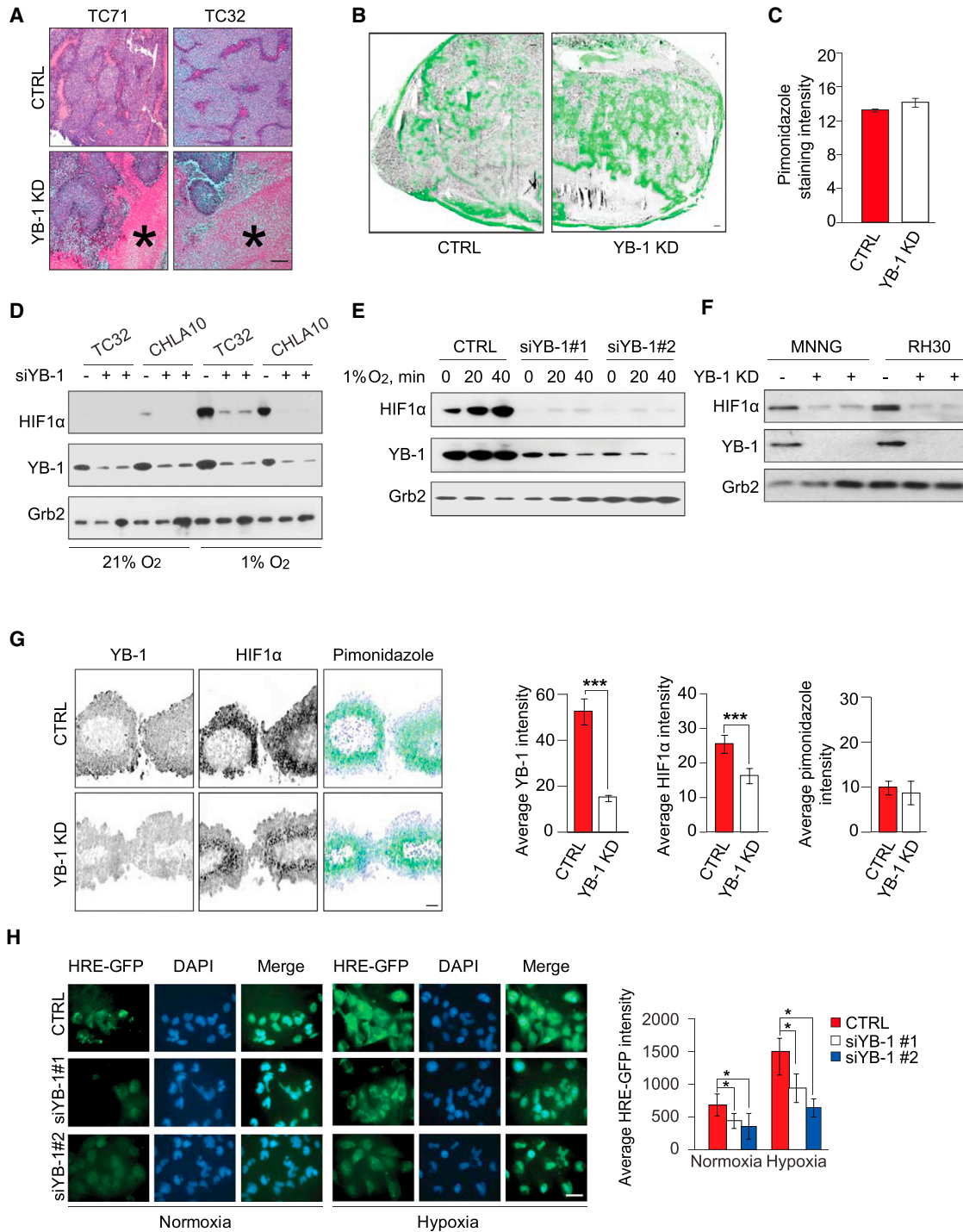


Figure 4. YB-1 Is Associated with Increased HIF1 α Protein Expression in Sarcoma Cells

(A) H&E-stained renal subcapsular tumor xenografts of TC71 and TC32 EWS cells \pm shRNA YB-1 KD. Asterisks show areas of necrosis. Scale bars represent 100 μ m.

(B) Assessment of hypoxia in MNNG tumor xenografts using pimonidazole hydrochloride. Pimonidazole was injected 90 min prior to sacrifice and stained in cryosections using pimonidazole antibodies to highlight hypoxic areas (green). Scale bars represent 150 μ m.

(C) Pimonidazole staining within tumors of (B) were quantitated as group averages \pm SEM for the sample mean, whereby whole tissue sections were analyzed for each tumor (n = 8 per group).

(D) Western blot of HIF1 α expression in TC32 and CHLA10 cells \pm siRNA YB-1 KD grown under normoxia or hypoxia (1% O₂) for 4 hr. Grb2 was used as a loading control.

(E) Western blot of HIF1 α and YB-1 expression in MNNG cells \pm YB-1 KD grown under hypoxia for the indicated time points. Grb2 was used as a loading control.

(legend continued on next page)

WT 5'-UTR, Δ 131–253 was less efficient, particularly at higher concentrations (Figure 5H; compare supershifted bands in lanes 7 versus 9). While not definitive, this further supports a role for nucleotides 131–254 (containing the majority of CG islands) in YB-1 binding to the *HIF1A* 5'-UTR. Together, these data strongly support a role for YB-1 in translational activation of *HIF1A*, likely through direct effects of YB-1 on *HIF1A* mRNA translational efficiency.

YB-1 Regulates HIF1 α Expression Independently of VHL

To assess potential effects of YB-1 on HIF1 α protein stability, we treated CHLA10 cells with cycloheximide to block translation and measured HIF1 α degradation rates. As shown in Figures 6A and 6B, degradation rates were unchanged between control and YB-1 KD cells, arguing against YB-1 regulating HIF1 α protein stability. Moreover, the MG132 proteasome inhibitor failed to completely rescue HIF1 α protein levels under normoxia in CHLA10 cells with YB-1 KD (Figure S6A), and YB-1 KD did not affect components of the Elongin B/C-CUL2-VHL (ECV) E3 ligase complex (Figure S6B), which targets HIF1 α for proteasomal degradation (Ivan et al., 2001; Jaakkola et al., 2001). To rigorously rule this out, we tested whether YB-1 could regulate HIF1 α protein expression in RCC4 renal carcinoma cells. These cells stabilize HIF1 α due to inactivation of the ECV E3 ligase through loss-of-function mutations of *VHL* (Maxwell et al., 1999). YB-1 KD in RCC4 cells led to marked loss of HIF1 α protein expression under both normoxia and hypoxia, as well as in RCC4 cells with reconstituted expression of functional *VHL* (Figure 6C). This provides compelling evidence that YB-1 regulation of HIF1 α protein levels in tumor cells is independent of the ECV HIF1 α E3 ligase. To test whether YB-1 regulates HIF1 α in other epithelial tumors, we performed YB-1 KD with two independent siRNAs (Figure S6C) under both normoxia and hypoxia in diverse epithelial tumor cell lines. YB-1 KD markedly reduced HIF1 α expression under hypoxia in prostate carcinoma (PC3 and LNCap) but not benign prostate epithelial cells (BPH1; Figure S6D), and in melanoma (MeWo), lung carcinoma (H1299), and breast carcinoma cells (MDA-MB-231, MCF7, and T47D; Figure S6E). While YB-1 is expressed in hypoxic non-tumorigenic human embryonic kidney HEK293 cells (Figure S6F) and normal fibroblasts (data not shown), this was not linked to increased HIF1 α protein induction in these cells, which along with the above BPH1 results, point to a specific role of YB-1 in regulating HIF1 α in transformed cells. Finally, we overexpressed Myc-tagged YB-1 in HeLa cervical carcinoma cells, which moderately but significantly enhanced HIF1 α expression under hypoxia compared with vector alone cells (Figure S6G; compare bars in the right). Together, these data strongly support a role for YB-1 in translational activation of *HIF1A* independent of the ECV E3 ligase and indicate that YB-1 regulation of HIF1 α pro-

tein expression is also functional in epithelial tumors in addition to sarcomas.

HIF1 α Is a Critical Effector of YB-1-Mediated Sarcoma Invasion and Metastasis

We next assessed whether HIF1 α is important for YB-1-induced invasion and metastasis of sarcoma cells. HIF1 α KD with two independent siRNAs in YB-1-competent MNNG cells (Figure S7A) significantly inhibited in vitro invasion under both normoxia and hypoxia and to a similar extent as YB-1 KD (Figure 7A). We then expressed either WT HIF1 α or the HIF1 α P402A/P564A Pro-to-Ala double mutant (resistant to HIF1 α degradation) (Masson et al., 2001) in MNNG YB-1 KD cells (Figure S7B). Expression of either isoform almost completely rescued invasive capacity of YB-1 KD cells under both normoxia and hypoxia (Figure 7B), highlighting HIF1 α as a critical in vitro effector of YB-1-mediated sarcoma cell invasion. To assess this in vivo, we ectopically expressed HIF1 α in CHLA10 and MNNG cells with stable YB-1 KD and monitored morphology of renal subcapsular xenograft tumors. YB-1 KD tumors again showed extensive hemorrhage and necrosis, which was almost completely rescued by HIF1 α re-expression (compare Figures 7Ca–f and see Figure S7C). Expression levels of YB-1 and HIF1 α were determined by IHC as above (Figures 7Cg–r). We then determined whether HIF1 α re-expression could rescue pulmonary dissemination of YB-1 KD cells in this model. While YB-1 KD again dramatically reduced metastatic capacity, this property was significantly increased in the same cells re-expressing HIF1 α (Figures 7Cs–aa and 7D). By comparison, YB-1 overexpression in CHLA10 cells (see Figures S3I and S4H) did not alter their metastatic capacity (see Figure 3G), likely because this led to only slight increases in HIF1 α in vivo (Figure S7D). Finally, to confirm HIF1 α functionality in this system, we examined expression of CAIX, a well-established HIF1 α target (Wykoff et al., 2000). CAIX expression was significantly reduced in MNNG tumors with YB-1 KD, but expression was rescued by HIF1 α re-expression in the same cells (Figure 8A). Moreover, since HIF1 α is a major driver of angiogenesis (Semenza, 2008) and because YB-1 KD increases hemorrhage and necrosis in xenografts (Figure 4A), we also assessed tumor microvessel density in EWS cell line xenografts \pm YB-1 KD, using IHC for the endothelial marker, CD31. This revealed highly significant decreases in CD31 staining and mean microvessel density in tumors derived from YB-1 KD compared to control cell lines (Figure 8B). This was confirmed using other blood vessel markers, namely endoglin (Figure S8A) and CD34 (Figure S8B). Ectopic HIF1 α expression in YB-1 KD tumor xenografts rescued blood vessel formation (Figure 8C). Together, these data show that YB-1 induces functionally active HIF1 α in vivo and highlight HIF1 α as a major effector of YB-1-mediated metastatic capacity of sarcoma cells.

(F) Effects of independent siRNAs targeting YB-1 (#1 and #2) on HIF1 α protein levels in the indicated cell lines incubated overnight at 0.2% O₂. Grb2 was used as a loading control.

(G) 3D tissue discs of MNNG cells were grown on collagen-coated tissue culture inserts for 16 hr prior to their transfer to stirred growth vessels. Cryosections from tissue discs were examined by IHC for YB-1, HIF1 α , and pimonidazole (scale bars represents 150 μ m), and staining intensities were quantified (mean \pm SD).

(H) HRE-GFP activity in RH30 RMS cells \pm siRNA YB-1 KD under normoxia and 1% O₂ (24 hr) was detected by fluorescence microscopy (scale bars represent 50 μ m) and quantified (mean of five fields \pm SD).

*p < 0.05, ***p < 0.001. See also Figure S4.

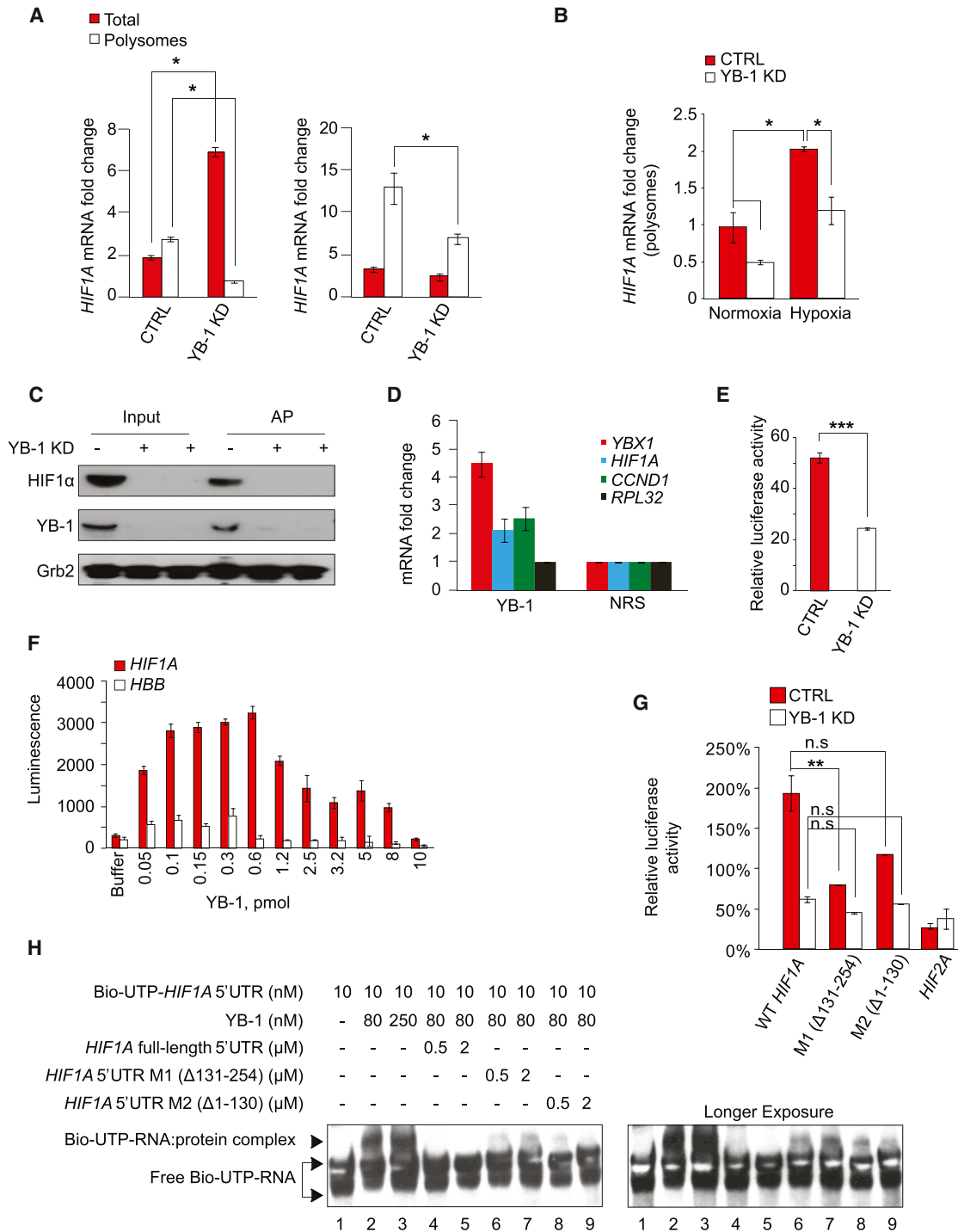


Figure 5. YB-1 Translationally Activates HIF1A Transcripts in Sarcoma Cells

(A) *HIF1A* mRNA expression in RH30 (left) and MNNG cells (right) ± siRNA YB-1 KD grown under normoxia (4 hr), as measured by qRT-PCR of total or polysomal fractionated RNA. Values were normalized against *GAPDH* from two experiments performed in triplicate and are presented as means ± SD.

(B) Total and polysomal *YBX1* and *HIF1A* mRNA levels in MG63 cells ± siRNA YB-1 KD grown under normoxia or 1% O₂ (4 hr), as measured by qRT-PCR. Values were normalized against *GAPDH* from two runs performed in triplicate and are presented as means ± SD.

(C) Affinity purification of biotinylated L-azidohomoalanine (AHA)-labeled acutely synthesized proteins from cell lysates ± YB-1 KD. Purified HIF1α and YB-1 proteins were then immunoblotted as indicated. Grb2 was used as a loading control.

(D) Fold change of *HIF1A* mRNA bound to YB-1 as measured by qRT-PCR following YB-1 immunoprecipitation. Controls include known YB-1 bound transcripts, *YBX1* and *CCND1*, and a known non-YB-1 binding transcript, *RPL32*. Values are normalized against *XIAP* from two runs in triplicate and presented as means ± SD. Normal rabbit serum (NRS) was used as an immunoprecipitation control.

(legend continued on next page)

DISCUSSION

Modern multi-agent chemotherapy and radiation regimens have markedly improved outcomes for localized forms of high-risk sarcomas such as EWS, OS, and RMS. However, the prognosis for patients with metastatic disease remains dismal, with almost no improvements in outcome for the past 20 years. While gene fusions have been identified in many sarcomas, these are present in both localized and widespread disease and thus do not account for metastatic behavior. YB-1 protein levels are markedly elevated in EWS, RMS, and OS, and expression correlates with poor outcome and metastatic disease. Moreover, YB-1 facilitates sarcoma cell invasive and metastatic capacity through direct binding to and translational activation of *HIF1A* mRNA, highlighting YB-1 as an invasion and metastasis factor in high-risk sarcomas through translational upregulation of HIF1 α .

Hypoxia plays a dominant role in tumor invasion and metastasis (Finger and Giaccia, 2010). Moreover, both YB-1 and HIF1 α promote metastatic dissemination in diverse cancers (Evdokimova et al., 2009; Gluz et al., 2009; Lee et al., 2009), potentially through common mediators such as Twist (Evdokimova et al., 2009; Yang et al., 2008), including sarcomas (Eisinger-Mathason et al., 2013). However, a link between YB-1 and HIF1 α has not been established. Prior studies of HIF1 α regulation under hypoxia have largely focused on transcriptional activation or protein stabilization. Stress-induced translation of HIF1 α remains poorly understood, even though it may play a critical regulatory role under hypoxia (Hui et al., 2006). YB-1 is a prominent RNA-binding protein and a well-established regulator of mRNA translation (Eliseeva et al., 2011). We show that YB-1 directly binds to the *HIF1A* 5'-UTR, that *HIF1A* transcripts are enriched in polysomes of control versus YB-1 KD sarcoma cells, and that YB-1 dramatically enhances acute synthesis of HIF1 α . Since the *HIF1A* 5'-UTR contains complex stem loop structures similar to those of *SNAI1*, it is likely that by binding to 5'-UTR secondary structures, YB-1 unwinds these structures to increase translational efficiency, as we reported for YB-1 induction of *SNAI1* and *TWIST* translation (Evdokimova et al., 2009).

Our study suggests that YB-1-mediated *HIF1A* mRNA translation occurs under both normoxia and hypoxia. Indeed, YB-1 is still required for HIF1 α protein expression even when HIF1 α is stabilized under normoxia in RCC4 cells, which lack VHL (Maxwell et al., 1999). It was previously reported that translation of *HIF1A* mRNA is enhanced under hypoxia in a 4EBP1/eIF4G-dependent and cap-independent manner, while translation of

mRNAs essential for proliferation is largely inhibited (Braunstein et al., 2007). YB-1-mediated *HIF1A* translation may be distinct from this process, given its activity under both normoxia and hypoxia, and may represent a more general mechanism that tumor cells can use to maintain HIF1 α levels. HIF1 α accumulation would then be further amplified under hypoxia through inactivation of prolyl hydroxylase activity (Kaelin, 2011).

YB-1 did not influence *HIF2A* translation or protein levels, even though the *HIF2A* 5'-UTR is also predicted to contain complex secondary structures. Using the above Vienna prediction tool, the calculated melting temperature for the *HIF1A* 5'-UTR is -115.59 kcal/mol compared with -198.53 kcal/mol for the *HIF2A* 5'-UTR. Therefore, one explanation for this discrepancy is that YB-1 is unable to melt the more stable *HIF2A* 5'-UTR and thus fails to promote *HIF2A* translation. Alternatively, sequence differences may preclude binding of YB-1 to the *HIF2A* 5'-UTR, and additional studies are required to address this question. Separate translational regulation of *HIF1A* and *HIF2A* might be advantageous to cells for maintaining independent control of *HIF1A* and *HIF2A* target genes.

Independent of effects on proliferation, YB-1 KD dramatically reduced invasion and metastatic capacity of sarcoma cells implanted under the renal capsules of immunocompromised mice, which was rescued by re-expression of HIF1 α . However, our studies do not rule out roles for other YB-1 translational targets. For example, YB-1 promotes translation of *TWIST* (Evdokimova et al., 2009). Moreover, *TWIST* is transcriptionally activated by HIF1 α in epithelial tumor cells, leading to increased metastasis (Yang et al., 2008). Expression of *TWIST* is reported in human sarcomas, but in association with an alternative mechanism of p53 inactivation in p53 WT leiomyosarcomas and liposarcomas, rather than with increased invasiveness (Piccinin et al., 2012). Moreover, we failed to detect a consistent link between YB-1 and *TWIST* expression in EWS, OS, and RMS. YB-1 also translationally regulates *TGFB1* mRNA (Fraser et al., 2008), known to mediate EMT and cancer metastasis (Taylor et al., 2013). Further studies are required to explore how these and other YB-1 translational targets might contribute to YB-1-mediated sarcoma metastasis.

In summary, these studies highlight a mechanism for HIF1 α regulation in high-risk sarcomas through YB-1-mediated translation, which contributes to metastasis in these diseases. YB-1 may therefore represent an exciting target for therapeutic intervention in sarcomas. Alternatively, targeting HIF1 α itself or its downstream effectors may offer more tractable clinical

(E) Translational efficiency of a bicistronic mRNA reporter construct containing the full-length *HIF1A* 5'-UTR upstream of firefly LUC, and Renilla LUC driven by simian virus 40 (SV40) promoter, in MNGG cells \pm YB-1 KD under normoxia. Results are displayed as means \pm SD from two independent experiments performed in triplicate.

(F) In vitro cell-free translation assay using reporter constructs with *HIF1A* or *HBB* 5'-UTRs linked to the SP6 RNA polymerase promoter incubated with increasing amounts of recombinant YB-1 protein and assessed for LUC activity. Results are displayed as means \pm SD from two independent experiments performed in triplicate.

(G) A bicistronic mRNA reporter construct as in (E) containing the full-length *HIF1A* 5'-UTR, its mutants M1 (Δ 131–254 nt), M2 (Δ 1–130 nt), or the *HIF2A* 5'-UTR was used to assess translation efficiency in CHLA10 cells \pm YB-1 KD under 1% O₂ for 4 hr. Results are displayed as means \pm SD from two independent experiments performed in triplicate.

(H) Electrophoretic mobility gel shift assay (EMSA) to detect binding of recombinant YB-1 to the *HIF1A* 5'-UTR. (Left) Biotin end-tagged full-length *HIF1A* 5'-UTR probe (Bio-UTP-HIF1 α 5'-UTR) and unlabeled full-length *HIF1A* 5'-UTR (lanes 4 and 5) or 5'-UTR deletion mutants lacking nucleotides 131–254 (Δ 131–254; lanes 6 and 7) or 1–130 (Δ 1–130; lanes 8 and 9) were incubated with recombinant GST-YB-1. Double arrows show free probe (Bio-UTP-RNA) while the single arrowhead shows supershifted Bio-UTP-RNA probe/YB-1 complexes. (Right) Longer exposure of the same figure.

* $p < 0.05$; ** $p < 0.01$, *** $p < 0.001$. See also Figure S5.

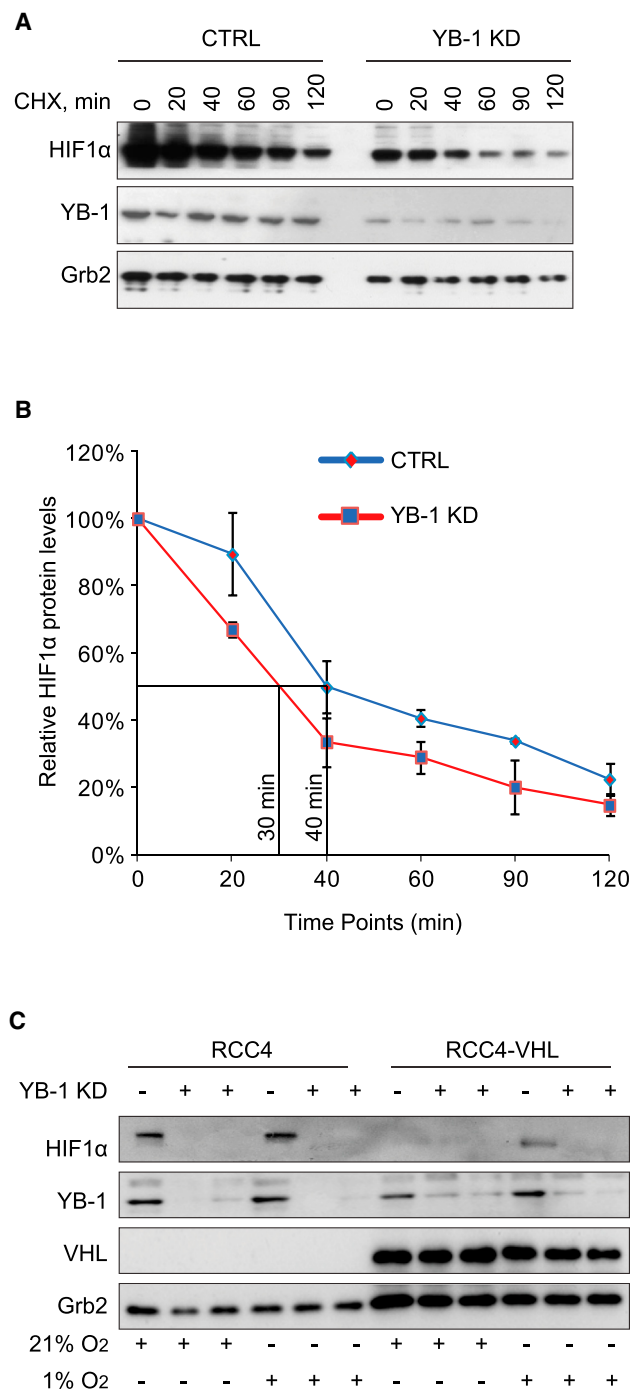


Figure 6. YB-1 Regulates HIF1 α Expression Independently of VHL

(A) Immunoblots showing HIF1 α protein decay in CHLA10 cells \pm YB-1 KD at the indicated time points after cyclohexamide (CHX) addition under 1% O₂. Grb2 was used as a loading control.

(B) Graphical representation of HIF1 α protein levels from (A) based on densitometry. Half-lives are shown under the curves, representing results of two independent experiments \pm SD.

(C) Western blots of HIF1 α , YB-1, and VHL expression in RCC4 (VHL-deficient) and RCC4-VHL (VHL re-expressed) cells \pm YB-1 KD with two independent siRNAs and grown under 21% or 1% O₂ for 4 hr as indicated. Grb2 was used as a loading control.

See also Figure S6.

strategies. Notably, effects of YB-1 on HIF1 α translation were not apparent in non-transformed cells, although the basis for this discrepancy remains unknown. Our observation that YB-1 also regulates HIF1 α protein levels in diverse epithelial tumor cell lines in an ECV E3 ligase-independent manner suggests that the proposed mechanism may be more broadly applicable in cancer biology. The xenograft systems we describe should provide robust preclinical models to evaluate HIF1 α pathway-targeting agents alone or in combination with other therapies to inhibit the spread of cancer cells mediated by YB-1.

EXPERIMENTAL PROCEDURES

Cell Lines

OB3 and OB5 primary OBs were developed as previously described (El Nagar et al., 2012). Primary human fibroblasts were kindly provided by Dr. Connie Eaves (University of British Columbia). RCC4 vector alone and RCC4-VHL cells were a kind gift of Dr. Michael Ohh (University of Toronto). The CHLA10 EWS cell line was kindly provided by Dr. Patrick Reynolds (Texas Tech University). TC71, TC32 EWS cell lines, and RH18 and RH30 RMS cell lines were gifts from Dr. Timothy Triche (Children's Hospital Los Angeles). Other cell lines were obtained from the American Type Culture Collection (ATCC). Culture conditions for each cell line are described in Supplemental Experimental Procedures.

Animal Studies

Murine renal subcapsular implantation studies were approved by the University of British Columbia Animal Care Committee, while zebrafish experiments were approved by the Dalhousie University Animal Care Committee. Detailed procedures are described in the Supplemental Experimental Procedures.

Ethics Approvals

IHC studies on human tissue samples were approved by the University of British Columbia Research Ethics Board (UBC REB Number H02-61375).

MCC System for 3D Cell Cultures

3D tissue discs were grown by seeding 1- to 4- μ l cells (500,000 cells/ μ l) into collagen-coated tissue culture inserts (CM 12 mm, pore size 0.4 μ m; Millipore). Seeded inserts were incubated for 16 hr and transferred to stirred growth vessels (Minchinton et al., 1997). Tissues were then grown for 5 days under 5% O₂, 5% CO₂ at 37°C. After 5 days, 100 μ M BrdU (Sigma) and 50 μ M pimonidazole (Hypoxyprobe) were added to label proliferation and hypoxia, respectively.

Western Blotting, Reagent, Immunofluorescence, and Antibodies

Western blotting and immunofluorescence were conducted using standard procedures. Human skeletal muscle tissue lysate was purchased from Abcam (Catalog number ab2933). Antibodies used are summarized in the Supplemental Experimental Procedures.

RNA Isolation and qRT-PCR

Total RNA was extracted as previously described (Peppel and Baglioni, 1990). Real-time quantitative PCR was performed using an ABI ThermoCycler (ABI Prism 7700 SDS). Human primers used are described in Supplemental Experimental Procedures.

HIF1 α Overexpression

Sarcoma cell lines \pm YB-1 KD were transfected with 500 ng of vector encoding WT or a degradation-resistant HIF1 α -P402A/P564A proline to alanine mutant, kind gifts of Dr. Thilo Hagen (University of Singapore) or empty vector using siLentFect. At 1-day post-transfection, cells were incubated under normoxia (21% O₂) or hypoxia (1% O₂) for 24 hr. Cells were then lysed and analyzed for HIF1 α expression by western blotting using Cayman HIF1 α rabbit polyclonal antibody.

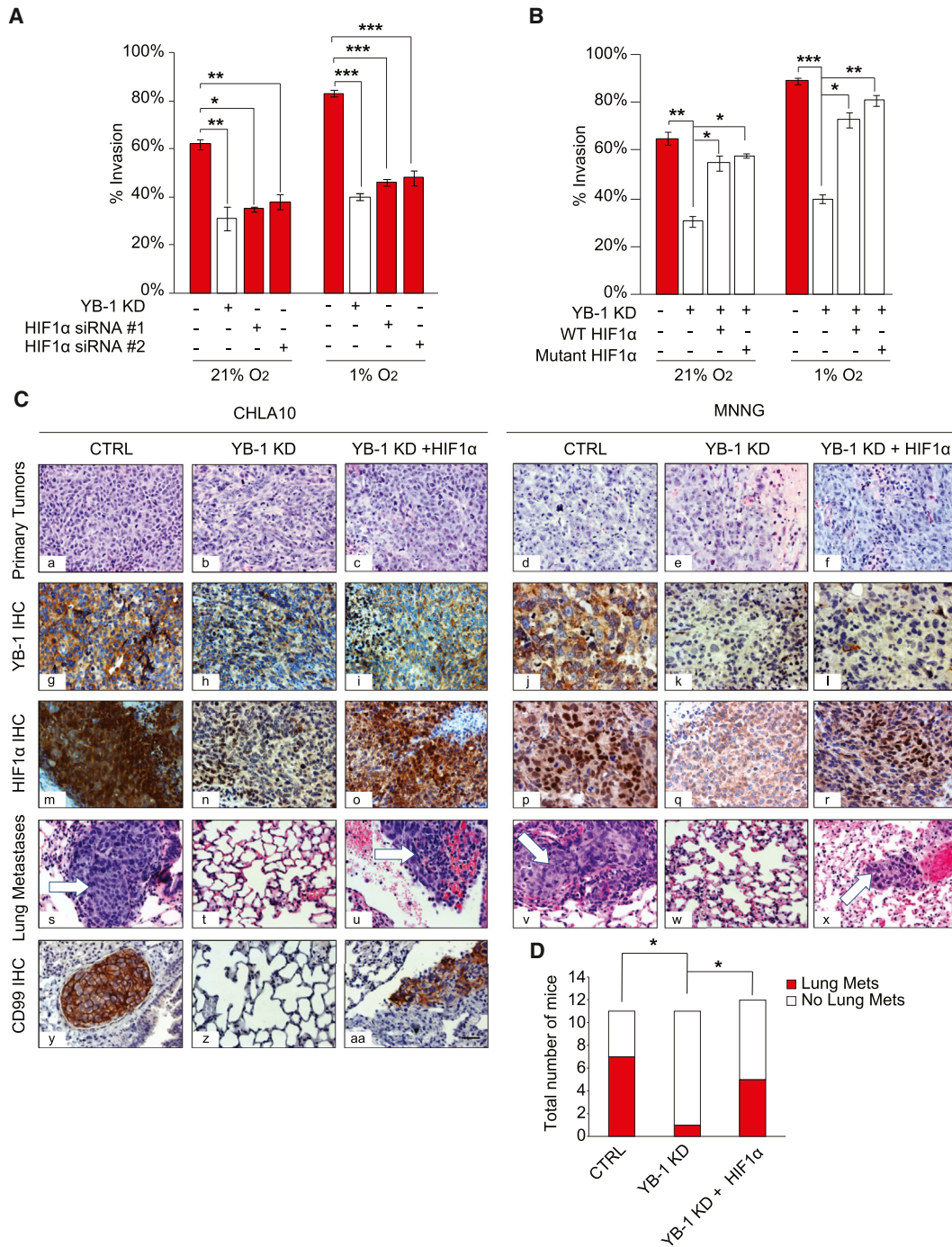


Figure 7. HIF1α Mediates the Invasive Phenotype of Sarcoma Cells

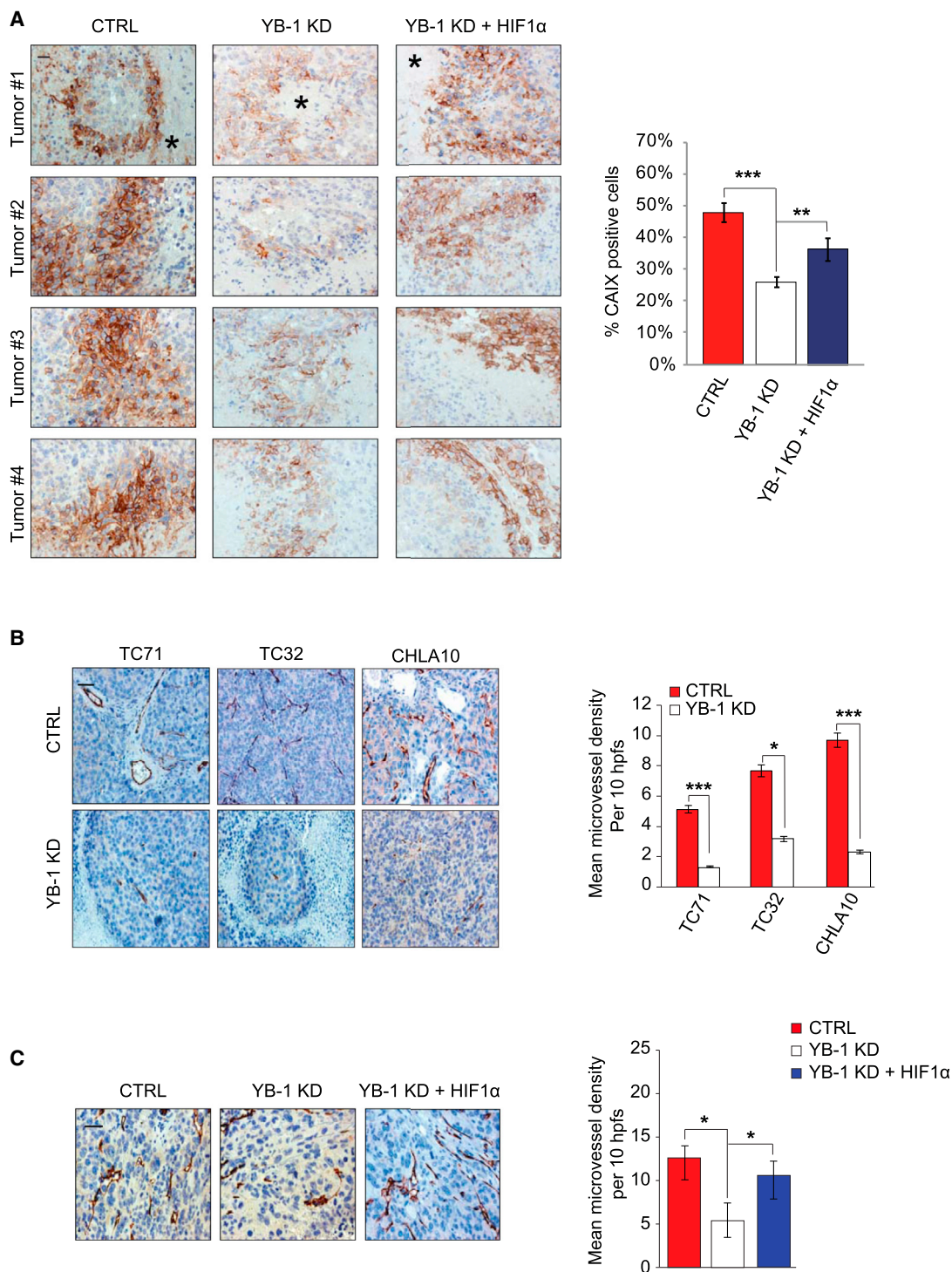
(A) Effects of YB-1 or HIF1α siRNAs KD on invasive capacity of MNNG cells under normoxia and 1% O₂ (8 hr) as assessed using in vitro invasion assays. Results are displayed as means ± SD from two independent experiments performed in triplicate.

(B) Effects of ectopic expression of WT or P402A/P564A mutant HIF1α on invasive capacity of MNNG cells with siRNA YB-1 KD under normoxia and 1% O₂ (8 hr), as assessed by in vitro invasion assays. Results are displayed as means ± SD from two independent experiments in triplicate.

(C) Primary tumors and lungs from mice bearing renal subcapsular tumor xenografts of CHLA10 and MNNG cell lines ± shRNA YB-1 KD and with or without ectopic WT HIF1α expression. (a–f) H&E staining of primary xenografts of the indicated cell lines. (g–l) IHC of YB-1 in primary xenografts. (m–r) IHC of HIF1α in primary xenografts. (s–x) H&E staining of lung metastases (arrows) in the indicated mouse groups. (y–aa) IHC of the CD99 EWS marker in lungs of mice bearing CHLA10 tumor xenografts. Scale bars represent 100 μm.

(D) Total number of mice bearing CHLA10 or MNNG xenografts ± YB-1 KD that developed lung metastases compared with mice with xenografts of the same YB-1 KD cell lines but ectopically expressing WT HIF1α, as determined using a Fisher's exact test.

*p < 0.05, **p < 0.005, ***p < 0.0005. See also Figure S7.



SUPPLEMENTAL INFORMATION

Supplemental Information includes Supplemental Experimental Procedures, eight figures, and three tables and can be found with this article online at <http://dx.doi.org/10.1016/j.ccell.2015.04.003>.

ACKNOWLEDGMENTS

We thank Drs. Valentina Evdokimova, Greg Goodall, Thilo Hagen, Peggy Olive, Catherine Pallen, Torsten Nielsen, Corinna Warburton, Yuanmei Lou, Steven Poon, Amy Li, and Brian Kwok for reagents, technical assistance, and helpful discussions. This work was supported by funds from the British Columbia Cancer Foundation through Team Finn and other generous riders in the Ride to Conquer Cancer (to P.H.S.), from Terry Fox Research Institute Team Grant 1021 (to P.H.S.), a Collaborative Health Research Project grant from the Canadian Institutes of Health Research and Natural Science and Engineering Research Council (to G.D. and J.N.B.), and support from C¹⁷ funding by the Ewings Cancer Foundation of Canada, Childhood Cancer Canada Foundation, and the Coast to Coast Against Cancer Foundation. A.M.E. was funded through a graduate scholarship from the Egyptian government, and D.P.C. was funded by the Beatrice Hunter Cancer Research Institute. K.L.B., a Michael Smith Foundation for Health Research Biomedical Research Scholar, was funded from the Canadian Institutes of Health Research.

Received: March 7, 2014
 Revised: February 28, 2015
 Accepted: April 10, 2015
 Published: May 11, 2015

REFERENCES

- Belaiba, R.S., Bonello, S., Zähringer, C., Schmidt, S., Hess, J., Kietzmann, T., and Görlach, A. (2007). Hypoxia up-regulates hypoxia-inducible factor-1 α transcription by involving phosphatidylinositol 3-kinase and nuclear factor kappaB in pulmonary artery smooth muscle cells. *Mol. Biol. Cell* **18**, 4691–4697.
- Bert, A.G., Grépin, R., Vadas, M.A., and Goodall, G.J. (2006). Assessing IRES activity in the HIF-1 α and other cellular 5' UTRs. *RNA* **12**, 1074–1083.
- Bogden, A.E., Haskell, P.M., LePage, D.J., Kelton, D.E., Cobb, W.R., and Esber, H.J. (1979). Growth of human tumor xenografts implanted under the renal capsule of normal immunocompetent mice. *Exp. Cell Biol.* **47**, 281–293.
- Braunstein, S., Karpisheva, K., Pola, C., Goldberg, J., Hochman, T., Yee, H., Cangiarella, J., Arju, R., Formenti, S.C., and Schneider, R.J. (2007). A hypoxia-controlled cap-dependent to cap-independent translation switch in breast cancer. *Mol. Cell* **28**, 501–512.
- Chaffer, C.L., and Weinberg, R.A. (2011). A perspective on cancer cell metastasis. *Science* **331**, 1559–1564.
- Corkery, D.P., Delleire, G., and Berman, J.N. (2011). Leukaemia xenotransplantation in zebrafish—chemotherapy response assay in vivo. *Br. J. Haematol.* **153**, 786–789.
- Cutz, J.C., Guan, J., Bayani, J., Yoshimoto, M., Xue, H., Sutcliffe, M., English, J., Flint, J., LeRiche, J., Yee, J., et al. (2006). Establishment in severe combined immunodeficiency mice of subrenal capsule xenografts and transplantable tumor lines from a variety of primary human lung cancers: potential models for studying tumor progression-related changes. *Clin. Cancer Res.* **12**, 4043–4054.
- Eisinger-Mathason, T.S., Zhang, M., Qiu, Q., Skuli, N., Nakazawa, M.S., Karakasheva, T., Mucaj, V., Shay, J.E., Stangenberg, L., Sadri, N., Pure, E., Yoon, S.S., Kirsch, D.G., and Simon, M.C. (2013). Hypoxia-dependent modification of collagen networks promotes sarcoma metastasis. *Cancer Discov.* **3**, 1190–1205.
- El Naggar, A., Clarkson, P., Zhang, F., Mathers, J., Tognon, C., and Sorensen, P.H. (2012). Expression and stability of hypoxia inducible factor 1 α in osteosarcoma. *Pediatr. Blood Cancer* **59**, 1215–1222.
- Eliseeva, I.A., Kim, E.R., Guryanov, S.G., Ovchinnikov, L.P., and Lyabin, D.N. (2011). Y-box-binding protein 1 (YB-1) and its functions. *Biochemistry Mosc.* **76**, 1402–1433.
- Evdokimova, V.M., and Ovchinnikov, L.P. (1999). Translational regulation by Y-box transcription factor: involvement of the major mRNA-associated protein, p50. *Int. J. Biochem. Cell Biol.* **31**, 139–149.
- Evdokimova, V., Ovchinnikov, L.P., and Sorensen, P.H. (2006a). Y-box binding protein 1: providing a new angle on translational regulation. *Cell Cycle* **5**, 1143–1147.
- Evdokimova, V., Ruzanov, P., Anglesio, M.S., Sorokin, A.V., Ovchinnikov, L.P., Buckley, J., Triche, T.J., Sonenberg, N., and Sorensen, P.H. (2006b). Akt-mediated YB-1 phosphorylation activates translation of silent mRNA species. *Mol. Cell. Biol.* **26**, 277–292.
- Evdokimova, V., Tognon, C., Ng, T., Ruzanov, P., Melnyk, N., Fink, D., Sorokin, A., Ovchinnikov, L.P., Davicioni, E., Triche, T.J., and Sorensen, P.H. (2009). Translational activation of snail1 and other developmentally regulated transcription factors by YB-1 promotes an epithelial-mesenchymal transition. *Cancer Cell* **15**, 402–415.
- Finger, E.C., and Giaccia, A.J. (2010). Hypoxia, inflammation, and the tumor microenvironment in metastatic disease. *Cancer Metastasis Rev.* **29**, 285–293.
- Fraser, D.J., Phillips, A.O., Zhang, X., van Roeyen, C.R., Muehlenberg, P., En-Nia, A., and Mertens, P.R. (2008). Y-box protein-1 controls transforming growth factor-beta1 translation in proximal tubular cells. *Kidney Int.* **73**, 724–732.
- Fujiwara-Okada, Y., Matsumoto, Y., Fukushi, J., Setsu, N., Matsuura, S., Kamura, S., Fujiwara, T., Iida, K., Hatano, M., Nabeshima, A., et al. (2013). Y-box binding protein-1 regulates cell proliferation and is associated with clinical outcomes of osteosarcoma. *Br. J. Cancer* **108**, 836–847.
- Galbán, S., Kuwano, Y., Pullmann, R., Jr., Martindale, J.L., Kim, H.H., Lal, A., Abdelmohsen, K., Yang, X., Dang, Y., Liu, J.O., et al. (2008). RNA-binding proteins HuR and PTB promote the translation of hypoxia-inducible factor 1 α . *Mol. Cell. Biol.* **28**, 93–107.
- Giménez-Bonafé, P., Fedoruk, M.N., Whitmore, T.G., Akbari, M., Ralph, J.L., Ettlinger, S., Gleave, M.E., and Nelson, C.C. (2004). YB-1 is upregulated during prostate cancer tumor progression and increases P-glycoprotein activity. *Prostate* **59**, 337–349.
- Gluz, O., Mengers, K., Schmitt, M., Kates, R., Diallo-Danebrock, R., Neff, F., Royer, H.D., Eckstein, N., Mohrmann, S., Ting, E., et al. (2009). Y-box-binding protein YB-1 identifies high-risk patients with primary breast cancer benefiting from rapidly cycled tandem high-dose adjuvant chemotherapy. *J. Clin. Oncol.* **27**, 6144–6151.
- Gupta, G.P., and Massagué, J. (2006). Cancer metastasis: building a framework. *Cell* **127**, 679–695.
- HaDuong, J.H., Martin, A.A., Skapek, S.X., and Mascarenhas, L. (2015). Sarcomas. *Pediatr. Clin. North Am.* **62**, 179–200.
- Höckel, M., and Vaupel, P. (2001). Tumor hypoxia: definitions and current clinical, biologic, and molecular aspects. *J. Natl. Cancer Inst.* **93**, 266–276.
- Hsieh, A.C., Liu, Y., Edlind, M.P., Ingolia, N.T., Janes, M.R., Sher, A., Shi, E.Y., Stumpf, C.R., Christensen, C., Bonham, M.J., et al. (2012). The translational landscape of mTOR signalling steers cancer initiation and metastasis. *Nature* **485**, 55–61.
- Hui, A.S., Bauer, A.L., Striet, J.B., Schnell, P.O., and Czyzyk-Krzeska, M.F. (2006). Calcium signaling stimulates translation of HIF-1 α during hypoxia. *FASEB J.* **20**, 466–475.
- Ivan, M., Kondo, K., Yang, H., Kim, W., Valiando, J., Ohh, M., Salic, A., Asara, J.M., Lane, W.S., and Kaelin, W.G., Jr. (2001). HIF1 α targeted for VHL-mediated destruction by proline hydroxylation: implications for O₂ sensing. *Science* **292**, 464–468.
- Jaakkola, P., Mole, D.R., Tian, Y.M., Wilson, M.I., Gielbert, J., Gaskell, S.J., von Kriegsheim, A., Hebestreit, H.F., Mukherji, M., Schofield, C.J., et al. (2001). Targeting of HIF-1 α to the von Hippel-Lindau ubiquitylation complex by O₂-regulated prolyl hydroxylation. *Science* **292**, 468–472.

- Kaelin, W.G., Jr. (2011). Cancer and altered metabolism: potential importance of hypoxia-inducible factor and 2-oxoglutarate-dependent dioxygenases. *Cold Spring Harb. Symp. Quant. Biol.* 76, 335–345.
- Kohno, K., Izumi, H., Uchiyama, T., Ashizuka, M., and Kuwano, M. (2003). The pleiotropic functions of the Y-box-binding protein, YB-1. *Bioessays* 25, 691–698.
- Lagarde, P., Przybyl, J., Brulard, C., Pérot, G., Pierron, G., Delattre, O., Sciot, R., Wozniak, A., Schöffski, P., Terrier, P., et al. (2013). Chromosome instability accounts for reverse metastatic outcomes of pediatric and adult synovial sarcomas. *J. Clin. Oncol.* 31, 608–615.
- Lee, S.L., Rouhi, P., Dahl Jensen, L., Zhang, D., Ji, H., Hauptmann, G., Ingham, P., and Cao, Y. (2009). Hypoxia-induced pathological angiogenesis mediates tumor cell dissemination, invasion, and metastasis in a zebrafish tumor model. *Proc. Natl. Acad. Sci. USA* 106, 19485–19490.
- Man, T.K., Chintagumpala, M., Visvanathan, J., Shen, J., Perlaky, L., Hicks, J., Johnson, M., Davino, N., Murray, J., Helman, L., et al. (2005). Expression profiles of osteosarcoma that can predict response to chemotherapy. *Cancer Res.* 65, 8142–8150.
- Masson, N., Willam, C., Maxwell, P.H., Pugh, C.W., and Ratcliffe, P.J. (2001). Independent function of two destruction domains in hypoxia-inducible factor- α chains activated by prolyl hydroxylation. *EMBO J.* 20, 5197–5206.
- Maxwell, P.H., Wiesener, M.S., Chang, G.W., Clifford, S.C., Vaux, E.C., Cockman, M.E., Wykoff, C.C., Pugh, C.W., Maher, E.R., and Ratcliffe, P.J. (1999). The tumour suppressor protein VHL targets hypoxia-inducible factors for oxygen-dependent proteolysis. *Nature* 399, 271–275.
- Mendoza-Naranjo, A., El-Naggar, A., Wai, D.H., Mistry, P., Lazic, N., Ayala, F.R., da Cunha, I.W., Rodriguez-Viciana, P., Cheng, H., Tavares Guerreiro Fregnani, J.H., et al. (2013). ERBB4 confers metastatic capacity in Ewing sarcoma. *EMBO Mol. Med.* 5, 1019–1034.
- Minchinton, A.I., Wendt, K.R., Clow, K.A., and Fryer, K.H. (1997). Multilayers of cells growing on a permeable support. An in vitro tumour model. *Acta Oncol.* 36, 13–16.
- Peppel, K., and Baglioni, C. (1990). A simple and fast method to extract RNA from tissue culture cells. *Biotechniques* 9, 711–713.
- Piccinin, S., Tonin, E., Sessa, S., Demontis, S., Rossi, S., Pecciarini, L., Zanatta, L., Pivetta, F., Grizzo, A., Sonogo, M., et al. (2012). A “twist box” code of p53 inactivation: twist box: p53 interaction promotes p53 degradation. *Cancer Cell* 22, 404–415.
- Postel-Vinay, S., Véron, A.S., Tirode, F., Pierron, G., Reynaud, S., Kovar, H., Oberlin, O., Lapouble, E., Ballet, S., Lucchesi, C., et al. (2012). Common variants near TARDBP and EGR2 are associated with susceptibility to Ewing sarcoma. *Nat. Genet.* 44, 323–327.
- Semenza, G.L. (2003). Targeting HIF-1 for cancer therapy. *Nat. Rev. Cancer* 3, 721–732.
- Semenza, G.L. (2008). Hypoxia-inducible factor 1 and cancer pathogenesis. *IUBMB Life* 60, 591–597.
- Semenza, G.L. (2014). Oxygen sensing, hypoxia-inducible factors, and disease pathophysiology. *Annu. Rev. Pathol.* 9, 47–71.
- Somasekharan, S.P., Stoyanov, N., Rotblat, B., Leprieux, G., Galpin, J.D., Ahern, C.A., Foster, L.J., and Sorensen, P.H. (2012). Identification and quantification of newly synthesized proteins translationally regulated by YB-1 using a novel Click-SILAC approach. *J. Proteomics* 77, e1–e10.
- Taylor, M.A., Sossey-Alaoui, K., Thompson, C.L., Danielpour, D., and Schieman, W.P. (2013). TGF- β upregulates miR-181a expression to promote breast cancer metastasis. *J. Clin. Invest.* 123, 150–163.
- Thoreen, C.C., Chantranupong, L., Keys, H.R., Wang, T., Gray, N.S., and Sabatini, D.M. (2012). A unifying model for mTORC1-mediated regulation of mRNA translation. *Nature* 485, 109–113.
- Wykoff, C.C., Beasley, N.J., Watson, P.H., Turner, K.J., Pastorek, J., Sibtain, A., Wilson, G.D., Turley, H., Talks, K.L., Maxwell, P.H., et al. (2000). Hypoxia-inducible expression of tumor-associated carbonic anhydrases. *Cancer Res.* 60, 7075–7083.
- Xu, M., Jin, H., Xu, C.X., Sun, B., Song, Z.G., Bi, W.Z., and Wang, Y. (2014). miR-382 inhibits osteosarcoma metastasis and relapse by targeting Y box-binding protein 1. *Mol. Ther.* 23, 89–98.
- Yang, M.H., Wu, M.Z., Chiou, S.H., Chen, P.M., Chang, S.Y., Liu, C.J., Teng, S.C., and Wu, K.J. (2008). Direct regulation of TWIST by HIF-1 α promotes metastasis. *Nat. Cell Biol.* 10, 295–305.